Super Vision Model: What's Peking Robin Seeing?

Hiroaki Kotera; Kotera Imaging Laboratory, Chiba, Japan

Abstract

Unlike trichromatic human vision, birds are tetrachromats with the fourth UV cone. This paper discusses on "What spectra are visible to Peking robin?" Human can see the spectrum C^*_A called "fundamental" extracted from the input spectrum C through Matrix-R_A. As well, Peking robin can see the fundamental C^*_B extracted through the extended Matrix-R_B. Matrix-R_B is given by Peking robin's ROGU (Red Orange Green and UV) cone sensitivities. The super vision spectrum C^*_B projected onto FCS (Fundamental Color Space) spans up to 300~400 nm UV range

The key is not to estimate the original hyper spectra but to restore the low-dimensional spectra called "fundamental", truly visible to the tetrachromat. The model doesn't take care the "metameric black" component but tries to predict the fundamental C^*_B from sRGB camera images under D65.

The fundamental C^*_B can be restored if the input spectrum C is known, but not always. Since the fundamental C^*_A without "metameric black" carries the unique tri-stimulus value T_A, it's mathematically recovered from T_A by "pseudo-inverse" projection.

Hence, the fundamental C^*_B must be recovered from the tetra-stimulus value T_B. The model predicts T_B from T_A based on the bold hypothesis that T_B (ROGU) will change interlocking to T_A (RGB) for the common scene. The fundamental C^*_B is restored by the pseudo-inverse projection of predicted T_B. The paper verifies how the model recovers the fundamentals in comparison with the true UV flower's spectra and discusses how it works well or not.

Projection to Tetra-chromatic Color Space

Human vision captures *LMS* tri-stimulus value T_A for input spectrum C through color matching function A as

$$T_A = \begin{bmatrix} L & M & S \end{bmatrix}^t = A^t C;\ t = transpose$$
$$A = \begin{bmatrix} l(\lambda) & m(\lambda) & s(\lambda) \end{bmatrix} \tag{1}$$
$$where,\ C = \begin{bmatrix} C(\lambda_1) & C(\lambda_2) & \cdots & C(\lambda_N) \end{bmatrix}^t$$

Based on *Matrix-R* theory, an input spectrum C is decomposed into low-dimensional component C_A^* plus residual K as

$$C = C_A^* + K$$
$$C_A^* = R_A C = R_A C_A^*,\ \ K = (I - R_A)C \tag{2}$$
$$R_A = A(A^t A)^{-1} A^t = R_A^n\ (n = 1, 2, ...\infty)$$

C_A^* is called "*fundamental*" or "*fundamental metamer*" and K is called "*metameric black*" (Cohen, *CRA,* 1988) [1][2].
C_A^* is visible spectrum to human vision, while K is invisible due to its zero tri-stimulus value $T_K = 0$.

Matrix-R_A is an identity-mapping operator which reflects the invariable human visual characteristics (Worthey, *CIC12*, 2004) [3].

While, Peking robin has tetra-chromatic four-band sensors of *ROGU* (*Red Orange Green and UV*) covering 300~700 nm[4].

Extending the matrix-R_A to the tetra-chromatic matrix-R_B, the projection of C onto 4D space of Peking robin is described by

$$T_B = \begin{bmatrix} R & O & G & U \end{bmatrix}^t = B^t C : tetra - stimulus\ value$$
$$C_B^* = R_B C :\ \ fundamental\ metamer$$
$$R_B = B(B^t B)^{-1} B^t\ \ for\ B = \begin{bmatrix} r(\lambda)\ o(\lambda)\ g(\lambda)\ u(\lambda) \end{bmatrix} \tag{3}$$
$$where,\ B\ denotes\ spectral\ sensitivities\ of\ ROGU$$

Figure 1 illustrates the differences between the tri-chromatic and tetra-chromatic vision systems. Here, the *LMS* cones spectral sensitivities in human vision are expanded to span the same wavelength range of 300~700 nm as Peking robin by setting null in the range of 300 ~ 400 nm.

It's notable that the projection matrix-R_B for Peking robin has four peaks different from matrix-R_A corresponding to *ROGU*. Based on the extended matrix-R_B, the *fundamental C_B^**, that is, spectra visible to Peking robin are obtained as given in Eq. (3).

Figure 2 compares the visible spectra to human vision and to Peking robin for EE (Equal Energy) white light stimulus. It shows how wide spectra Peking robin can see including *UV* range.
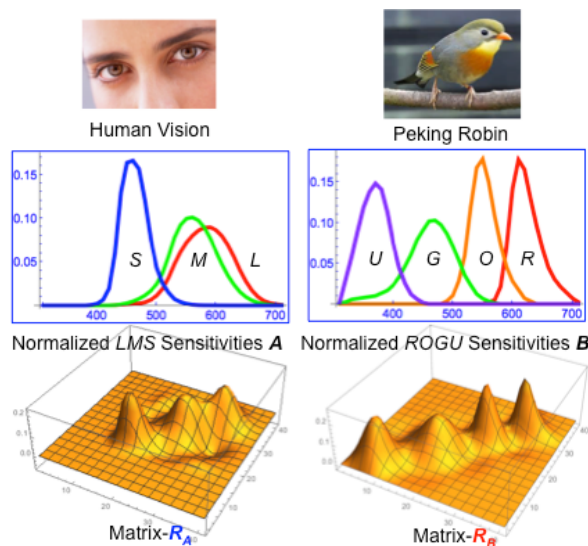
Figure 1. Matrix-R projectors created for Human Vision and Peking Robin
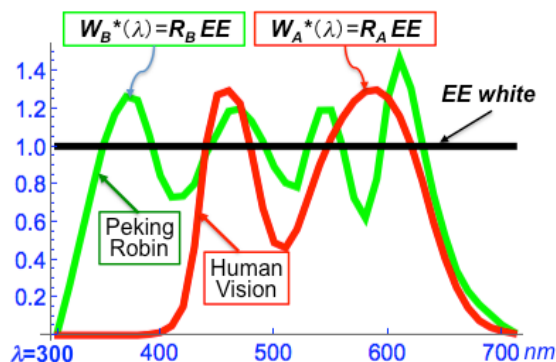
Figure 2. Visible spectra to Human Vision and to Peking Robin for EE White

Fundamental Color Space for Peking Robin

Based on the matrix-R_B, the 4-D FCS of Peking robin is constructed from the orthonormal basis function $F_B(\lambda)$ by

$$F_B(\lambda) = GramSchmidt\big[E_B\big]$$
$$for \ E_B = \big[W_B*, E_R, E_O, E_U\big]$$
$$W_B* = R_B EE(white), \ E_R = R_B^{row}(600nm),$$
$$E_O = R_B^{row}(540nm), \quad E_U = R_B^{row}(360nm)$$

(4)

According to the basic concept of FCS (Kotera, *AIC 2007*) [5], we can select arbitrary set of four row vectors in matrix-R_B, as a candidate for basis E_B. First, three single row vectors $\{E_R \ E_O \ E_U\}$ in matrix-R_B are selected at the peak of λ =600, 540, 360 nm for *ROU* cones. In addition, the *fundamental* W_B* for *EE* white is chosen as the forth entry in E_B instead of the basis for *G* cone. Since W_B* is the ensemble of all monochromatic *fundamentals* to reconstruct *EE* white, a complete OCS (Opponent Color Space) is created through *GramSchmidt* procedure (Kotera, *CIC 2014*)[6].

The basis matrix E_B and orthonormal basis function $F_B(\lambda)$ as a complete OCS are illustrated in *Figure 3* (a) and (b).

The FCS of Peking Robin has 4-D structure and chrominance bases 1, 2, and 3 span 3-D space quite different from 2-D of HVSS as roughly sketched by LUM in *Figure 3* (c).
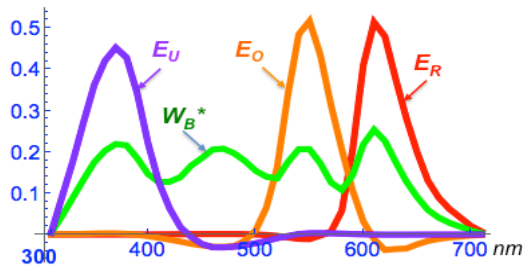
(a) *Set of selected fundamantals for the basis matrix E_B*
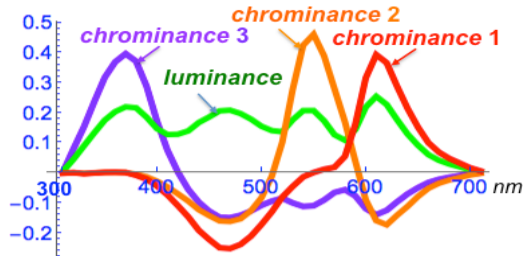
(b) *Orthonormal basis function $F_B(\lambda)$ for complete OCS*
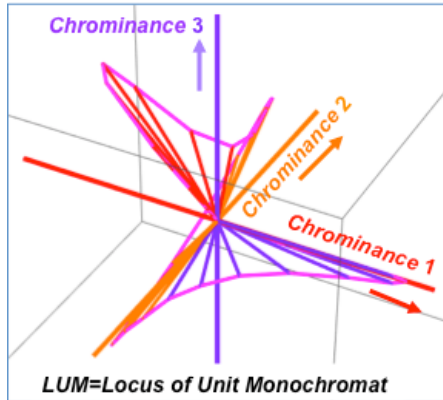
(c) *3-D Chrominance space sketched by LUM locus*

Figure 3. FCS spanned by tetra-chromatic bases for Peking Robin

Theoretical Estimation of Fundamentals

The major objective is to estimate the *fundamental C_B**, that is, the super vision spectra visible to Peking robin. The countless metamers exist, whose spectrum $C(\lambda)$ is different but has the same tri/tetra-stimulus value. It's notable that among them, only the *fundamantal $C_A*(\lambda)$* and $C_B*(\lambda)$ carry the unique T_A for human vision and unique T_B for Peking robin. Again, we should notice the *fundamental $C_B*(\lambda)$* is the visible spectrum to Peking robin.

Because $C_A*(\lambda)$ and $C_B*(\lambda)$ are equivalent to T_A and T_B, mathematically they are exactly restored from T_A and T_B by the pseudo-inverse projection (Kotera, *CIC 1996*) [7] as given by

$$C_A*(\lambda) \cong P_{INV}^A T_A, \quad P_{INV}^A = A(A^t A)^{-1}$$
$$C_B*(\lambda) \cong P_{INV}^B T_B, \quad P_{INV}^B = B(B^t B)^{-1}$$

(5)

Thus, theoretically, two ways exist to get the correct fundamentals, one by Eq. (3) and the other by Eq. (5). The paper uses the latter.

Approximation by LMS to ROGU Prediction

Human vision perceives color sensation by tri-stimulus value $T_A = A^t C$, while Peking Robin by tetra-stimulus value $T_B = B^t C$ for the same spectral input C. However, in general, C is unknown unless we use expensive hyper spectral camera covering $300 \sim 400$ nm *UV* range besides visible range. Here, we make an expectation of linear relation between T_A and T_B.

Supposing a human and a Peking robin are seeing the common scene in *Figure 4*, the following hypotheses look promising.

[HP1] *LMS* and *ROGU* cone sensors are linearly excited by the SPD (Spectral Power Distribution) of the objects in the scene.
[HP2] SPDs are smoothly and continuously spreading over *M-S* range of HVSS into *G-U* range of Peking robin.

Now, the model tries to estimate T_B from T_A by a simple linear transform with 4 x 3 matrix M_{43} as

$$T_B = \big[R,O,G,U\big]^t \cong M_{43} T_A = M_{43}\big[L,M,S\big]^t$$

(6)

Considering the relations of $T_A = A^t C$ and $T_B = B^t C$, we get

$$B^t = M_{43} A^t$$

(7)

Operating the color matching function A on both sides, we get

$$B^t A = M_{43}\big(A^t A\big) = M_{43} W_{33}, \ W_{33} = A^t A : constant$$
$$M_{43} = B^t A(A^t A)^{-1}$$

(8)

But, any restrictions are not considered in the simple Eq. (6). Taking the white balance into consideration, just as von Kries linear color adaptation model, matrix M_{43} in Eq. (6) is corrected to satisfy the following condition for Equal Energy white light *EE* as

$$_{EE}T_A = \big[L_{EE} \ M_{EE} \ S_{EE}\big]^t = A^t EE \cong \big[1 \ 1 \ 1\big]^t$$
$$_{EE}T_B = \big[R_{EE} \ O_{EE} \ G_{EE} \ U_{EE}\big]^t = {}_{COR}M_{43 \ EE}T_A \cong \big[1 \ 1 \ 1 \ 1\big]^t$$

(9)

Thus, Eq. (6) is rewritten with the corrected matrix $_{COR}M_{43}$ as

$$T_B = \big[R,O,G,U\big]^t \cong {}_{COR}M_{43} T_A = {}_{COR}M_{43}\big[L,M,S\big]^t$$

(10)

Using the spectral sensitivities of *ROGU*, the matrix $_{COR}M_{43}$ is calculated as

$$_{COR}M_{43} = B^t A(A^t A)^{-1} = \begin{bmatrix} 3.56382 & -2.64382 & 0.07999 \\ -1.08554 & 2.17902 & -0.09348 \\ -0.36565 & 0.46643 & 0.89922 \\ 0.51330 & -0.58934 & 1.07605 \end{bmatrix}$$

(11)
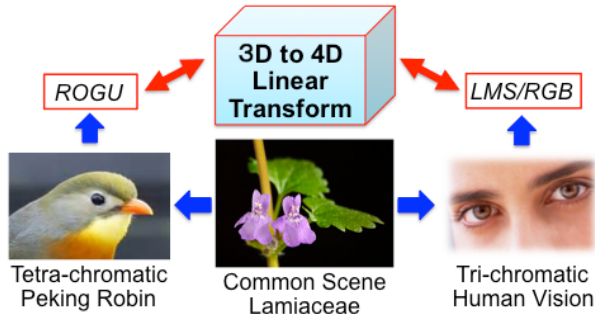
Figure 4. Linear model to bridge trichromatic and tetrachromatic visions

Simulation Results

Verification of Model with Known Spectra

In order to verify the proposed prediction model, some known spectral data are used and compared with the theoretical model. The true fundamental C^*_B visible to Peking robin is theoretically given with the *Matrix-R_B* in Eq. (3). The same C^*_B is also obtained with the pseudo-inverse operator P^B_{INV} in Eq. (5).

Figure 5 compares the fundamental spectra visible to Peking robin and human for typical UV flower "*Plumonaria Obscura*"[8]

Figure 6 shows the verified samples by a comparison between the estimation by models and by the theoretical calculation. It's notable that the linear predictions worked almost perfect for "*Plumonaria Obscura*" but imperfect for "*Opium Poppy*"[9].

As expected, **Panel A** by the *Matrix-R_B* and **Panel B** by the pseudo-inverse operator are perfectly coincided each other**.**

On the other hand, **Panel C** shows the results by the *LMS* to *ROGU* prediction model. Since any physical connections don't exist between the neural networks of human vision and Peking robin, the exact recovery of fundamentals from the low-dimensional *LMS* values may be a sort of ill-posed problem. Hence, the results in **Panel C** include some estimation errors. It's notable that the estimation was very accurate for "*Plumonaria Obscura*" but erroneous for "*Opium Poppy*" mostly in the UV range. The reason why is guessed coming from the difference in their SPDs. Since the SPD is strong in *M-S*/*Green-Blue* ranges for "*Plumonaria Obscura*", the above-mentioned hypothesis [**HP2**] is well satisfied. While, it's insufficient for "*Opium Poppy*", who's SPD in the same ranges is weak. In the linear prediction model from *LMS* to *ROGU*, the contribution of *M-S*/*Green-Blue* ranges to the *U* channel plays an important role.

Getting Peking Robin's UV-Band from sRGB Image

Since the *LMS* tri-stimulus value T_A is obtained by *sRGB* camera image through linear transform, the corresponding *ROGU* tetra-stimulus value T_B is predicted from T_A by Eq. (10). Once the tetra-stimulus value T_B is obtained, the *fundamental C^*_B* in each pixel is predicted by applying Eq. (5) again to it.

Figure 7 shows the procedure for getting the fundamentals $C_A^*(\lambda)$ and $C_B^*(\lambda)$ from sRGB image "*Commelina communis*" known as the Aslatic dayflower. It's shown that the *fundamental $C_B^*(\lambda)$* for Peking robin spans wider range than $C_A^*(\lambda)$ for human vision covering $300 \sim 400$ nm *UV*. The color separated *UV*-band image is visualized by colorizing to *Cyan* after normalizing. The petal area of flower seems to mainly reflect the *UV* spectra.

Figure 8 illustrates some examples for the estimated $C_A^*(\lambda)$ vs. predicted $C_B^*(\lambda)$ from sRGB images. The unique-shaped purple petals in "*Lamiaceae*"[10] strongly and selectively reflect the *UV*.
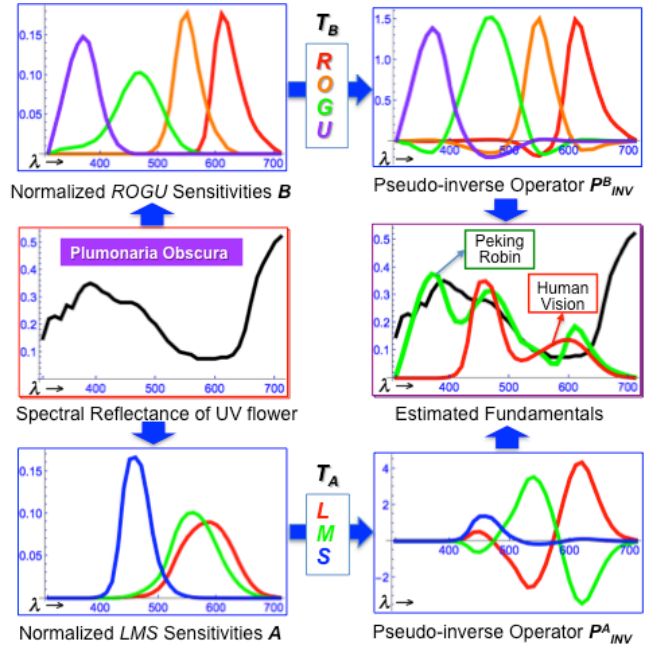
Figure 5. Comparison of Visible Spectra for "Plumonaria Obscura"

The other three samples are the bird's favorite berry or nut. Each displays its own *UV* reflections. Since the precise UV reflections are hardly reported from the Wild Bird Society of Japan, it's uncertain if they are growing stronger as getting ripe.

Comparison with UV Photography

Since we are blind to the *UV* spectra and hard to know what color sensations happen in the visual cortex of Peking robin, the question is how to verify the validity of proposed model.

One of the ways is to compare the estimated *U*-band image with that by *UV* photography. Typically there are two ways for *UV* photography by capturing the reflected *UV* light and the *UV* induced fluorescence. *UV* photographers are trying to visualize the hidden *UV*-marking of flowers and to create a variety of fantastic images invisible by normal photography. *UV* spectra are strongly absorbed in the center and reflected in the corolla (petal) of flower.

Recently a gear to take *UV* photos by digital camera is ready for amateur use, such as a kit of filters (*UV* bandpass, *IR* cut, *CC*: Color Compensation) with macro lens and *UV* flash lamp.

Figure 9 shows some examples in comparison with *UV* photographs. The sample (a) is "*Lamiaceae*" which is known as a typical *UV* flower taken by digital camera with *UV* filter and *UV* flash lamp. Since the *use of UV* flash lamp causes an induced fluorescence except reflection, the exact check is difficult against the estimated *U*-band image by proposed model. Though, the colorized "*cyan*" areas show that Peking robin is sensitive to the *UV* spectra mainly in the petals of "*Lamiaceae*". Roughly speaking, the estimated result corresponds to the *UV* photograph very well. The sample (b) is another comparison with a yellow butterfly taken by digital camera Nikon D80 with SIGMA macro lens and *UV* plus *IR* cut filters[11]. The *UV* image is extracted from *B*-channel and colorized to "*bluish*" using Adobe Photoshop and finally synthesized with normal *RGB* image. Also in this case, it's hard to make a quantitative evaluation, but the proposed model may be succeeded in visualizing the Peking robin's *UV* world to a certain degree.
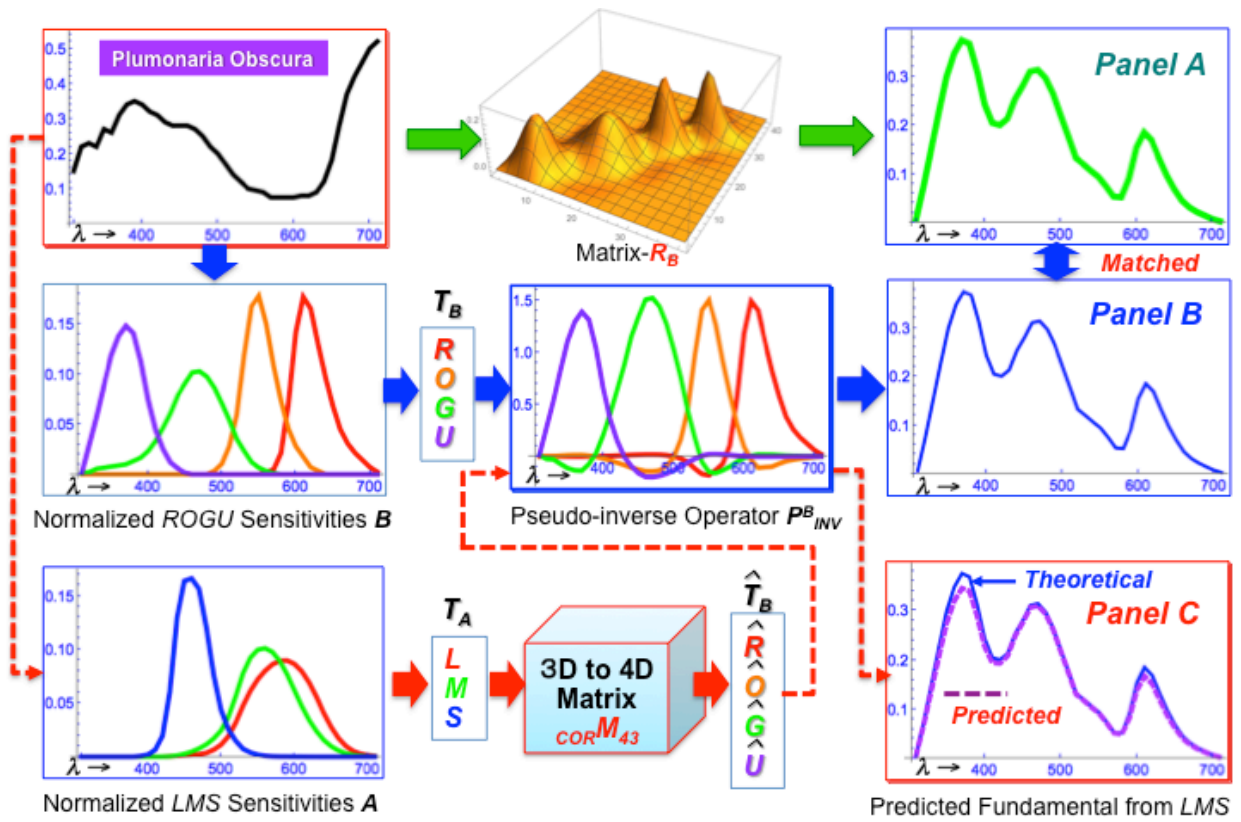
(a) *Estimated Super vision fundamental for Peking robin:* **Successful sample** *in case of* **"Plumonaria Obscura"**
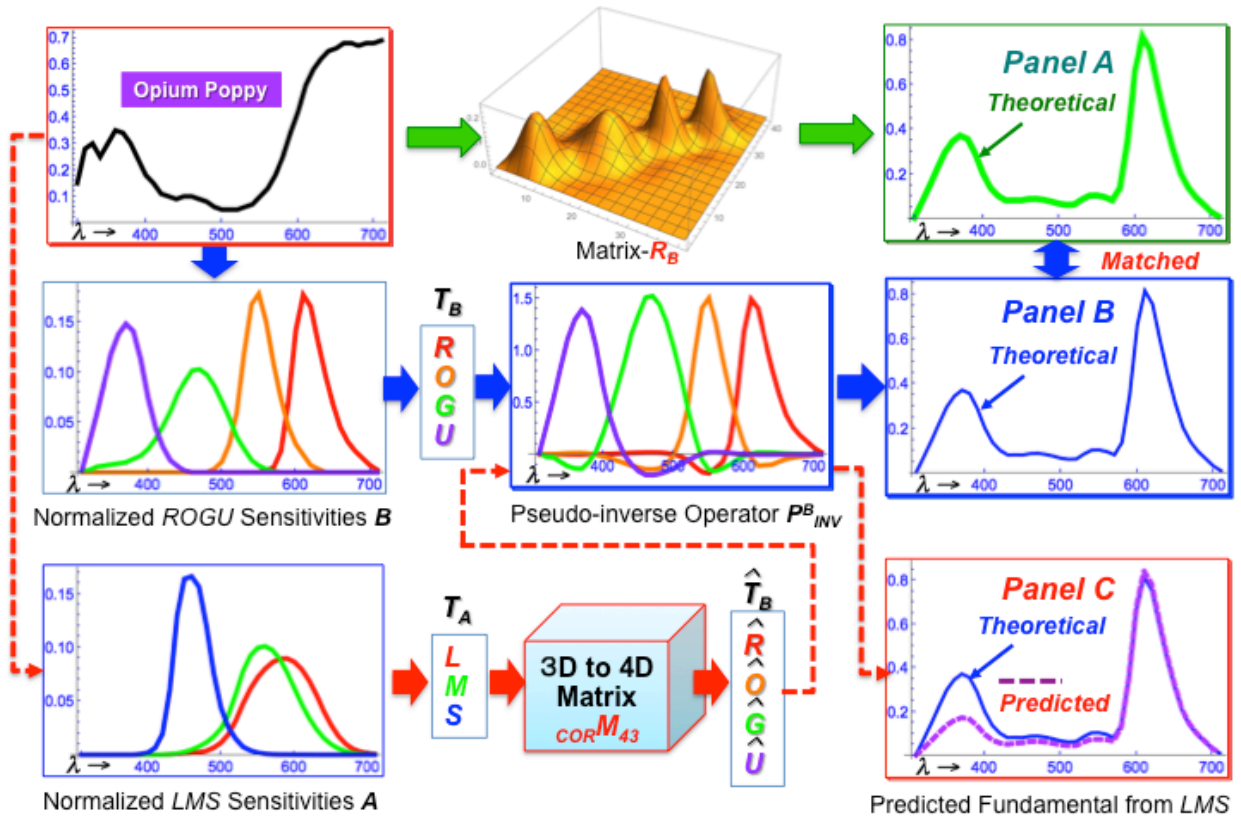
(b) *Estimated Super vision fundamental for Peking robin:* **Defective sample** *in case of* **"Opium Poppy"**

Figure 6. Estimated Fundamentals for known UV flowers spectra by linear prediction model in comparison with Theoretical model
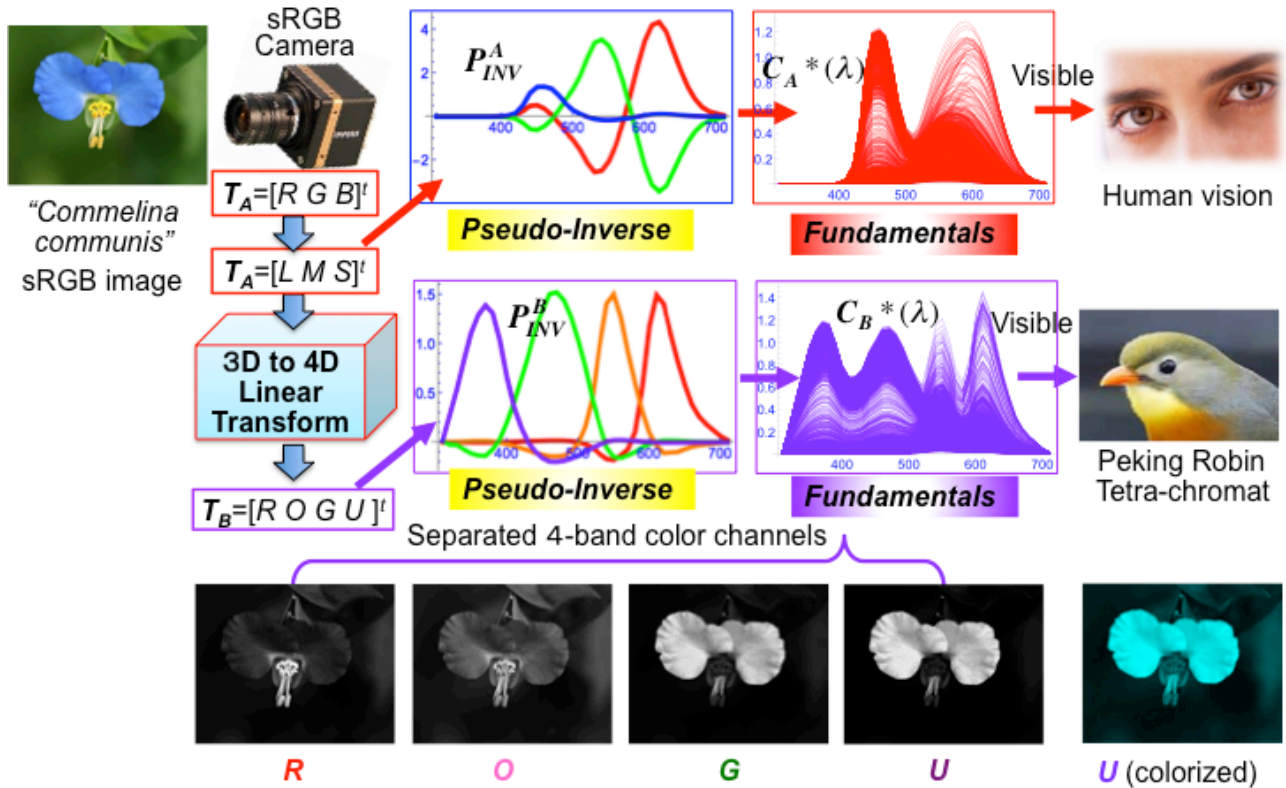
Figure 7. Procedure for estimating fundamentals and visualization of UV spectra visible to Peking robin from sRGB real scene
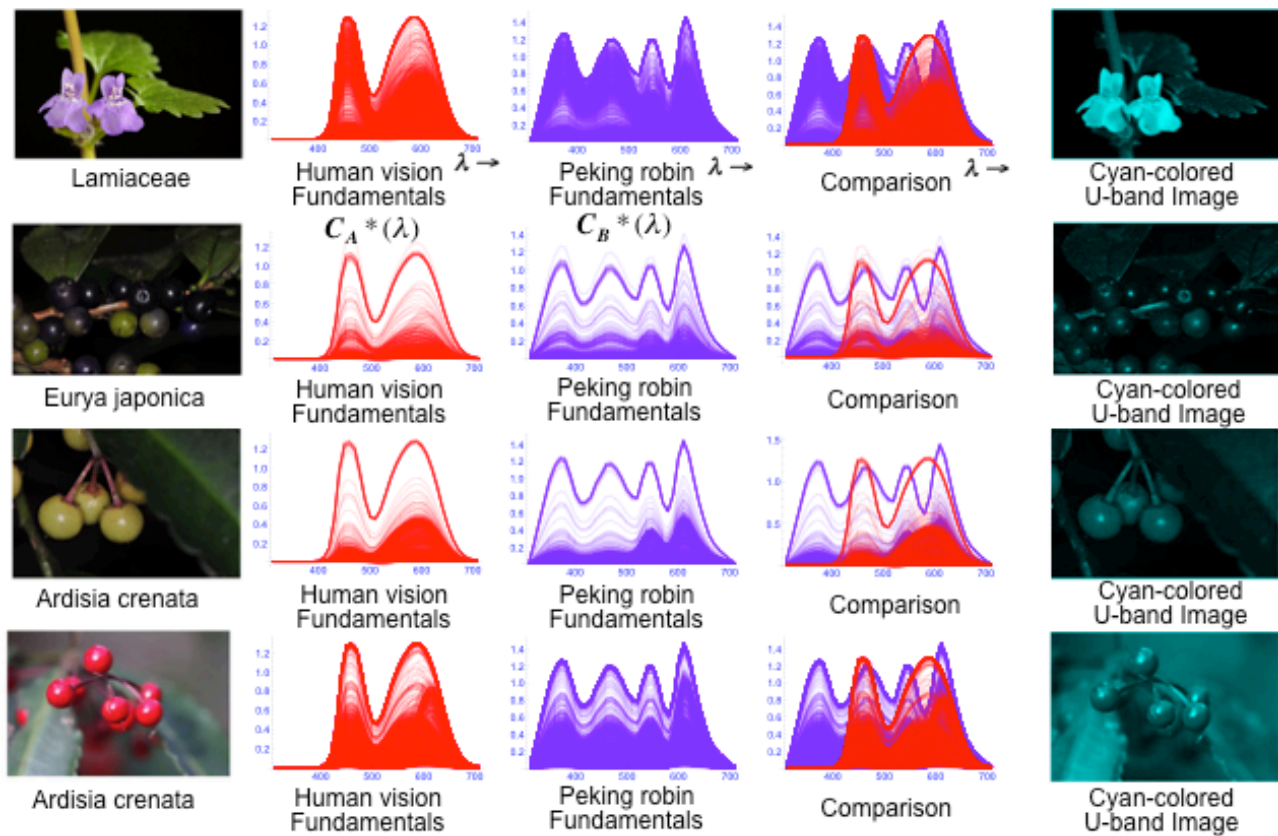
Figure 8. UV spectral images visible to Peking robin predicted from sRGB real scene
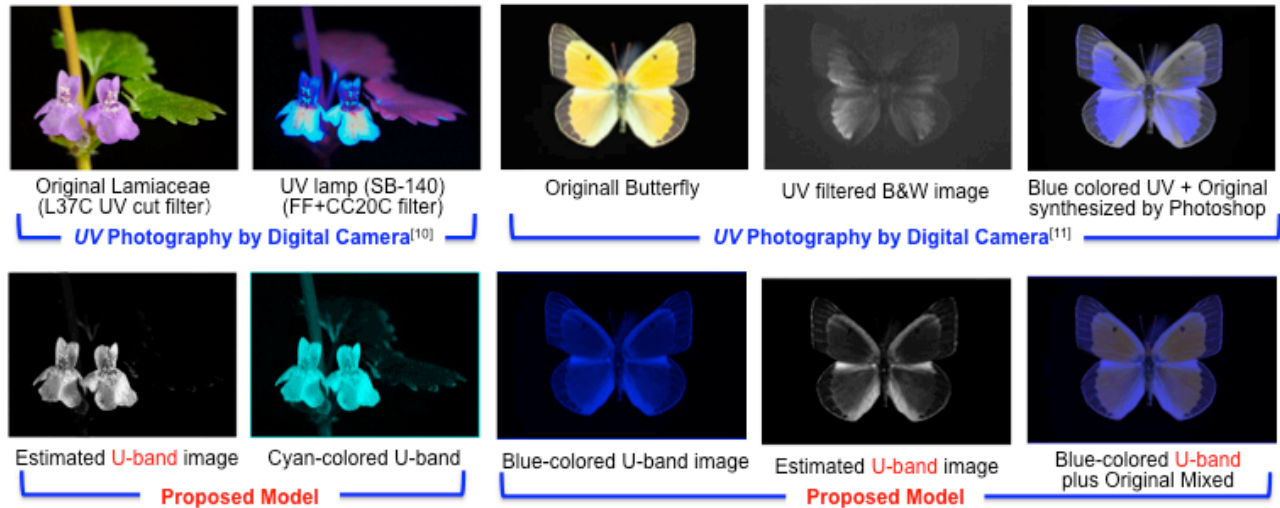
Figure 9. Predicted and Visualized UV images in comparison with UV photography

Discussion and Conclusions

Spectral imaging based on multi-band sensors are wide spread to a variety of industrial applications. The major objectives are mostly focused on the acquisition of faithful color information and archiving the cultural heritage, but mainly restricted in the visible spectral range of human vision. While, the imaging in the infrared spectral range has been applied to the remote sensing in weather and earth observation satellites, or public security system. On the other hand, the *UV* imaging is not so popular as compared with visible or *IR* imaging. But, except the medical application to skin care or skin cancer diagnostics, the targets may be spreading to a new field in the near future.

The birds find the ripe fruits quickly with *UV* sensor and the fruits reflect *UV* strongly as they go ripe to be eaten by birds and for the seeds to be scattered widely, that is, they have own color strategy for mutual help. The flowers absorb *UV* spectra strongly in the center and reflect in the petal to be easily found and pollinated by bees. The bees need to get foods quickly. *UV* imaging should be paid more attention from a point of natural environment protection.

This paper challenged to estimate the hyper spectral image just as viewed by tetra-chromatic Peking robin from the same sRGB image viewed by trichromatic human vision. The key point is not to estimate the original hyper spectra but to recover the essential low-dimensional spectra called *"fundamental",* truly visible to the tetrachromat based on the extended Matrix-***R*** theory.

The proposed model clarified
[1] Structure of Tetra-chromatic 4-D FCS
[2] Expensive multi-band camera is not necessary but popular sRGB camera is available for predicting the *UV*-band image.
[3] The estimated *UV* images proved to roughly correspond to those by *UV* photography.

Author Biography

*   **Hiroaki Kotera** *joined Panasonic in 1963. He received PhD from Univ. of Tokyo. After worked at Matsushita Res. Inst. Tokyo during 1973-1996, he was a professor at Chiba University. He retired in 2006 and is collaborating with Chiba University. He received 1993 IS&T honorable mention, 1995 SID Gutenberg prize, 2005 IEEE Chester Sall award, 2007 IS&T Raymond. C. Bowman award, 2009 SPSTJ and 2012 IIEEJ best paper awards. He is a Fellow of IS&T and IIEEJ.*

Strictly speaking, the results should be evaluated more rigorously in comparison with the accurate spectral images not the *UV* photographs, but the hyper spectral images covering 300 ~ 700 nm. If any multi-band hyper spectral image database including visible plus *UV* range of 300 ~ 400 nm are provided, the proposed model is ready for continuing the more reliable inspection and verification as a future work.

References
[1] J. B. Cohen: Color and Color Mixture: Scalar and Vector Fundamentals, *C. R. A.*, 13, 1, 5-39 (1988)
[2] J. B. Cohen: Visual Color and Color Mixture, Fundamental Color Space*, Illinois Press* (2002)
[3] J. A. Worthey et al: Camera Design Using Locus of Unit Monochromats, Proc. CIC12, 327-333 (2004)
[4] M. Vorobyev et al.: Tetrachromacy, oil droplets and bird plumage colors, *J. Comp. Physiol. A* 183, 621- 633 (1998)
[5] H. Kotera: Geometrical Structures of Fundamental Color Space, *Proc. AIC2007,* O2-08 (2007)
[6] H. Kotera: A Complete Opponent-Color Space with Golden Vectors, *Proc. CIC22,* 65-70 (2014)
[7] H. Kotera: Recovery of Fundamental Spectrum from Color Signals, *Proc. CIC4,* 141-144 (1996)
[8] L. Chittka et al.: Ultraviolet as a Component of Flower Reflections, and the Colour Perception of Hymenoptera, *Vision Res.*, 34, 11, 1489-1508 (1994)
[9] Arnold, S.E.J. et al.: The floral reflectance spectra database, *Nature Precedings* (2008) http://www.reflectance.co.uk/
[10] Bjørn Rørslett: Flowers in Ultra-Violet, http://www.naturfotograf.com/UV_flowers_list.html#ROSACEAX
[11] K. Shiraiwa: Pteron World, http://www.pteron-world.com/topics/photography/phototechnics-uv.html